

SimTO: A simulation-based topology optimization framework for bespoke soft robotic grippers

Kurt Enkera^{1,2*}, Josh Pinskier¹, Marcus Gallagher², David Howard¹

¹CSIRO Robotics, CSIRO, 1 Technology Ct, Brisbane, 4069, Queensland, Australia.

²School of Electrical Engineering and Computer Science, The University of Queensland, Sir Fred Schonell Drive, Brisbane, 4072, Queensland, Australia.

*Corresponding author(s). E-mail(s): kurt.enkera@csiro.au;

Contributing authors: josh.pinskier@csiro.au; marcusg@uq.edu.au;
david.howard@csiro.au;

Abstract

Soft robotic grippers are essential for grasping delicate, geometrically complex objects in manufacturing, healthcare and agriculture. However, existing grippers struggle to grasp *feature-rich* objects with high topological variability, including gears with sharp tooth profiles on automotive assembly lines, corals with fragile protrusions, or vegetables with irregular branching structures like broccoli. Unlike simple geometric primitives such as cubes or spheres, feature-rich objects lack a clear “optimal” contact surface, making them both difficult to grasp and susceptible to damage when grasped by existing gripper designs. Safe handling of such objects therefore requires *specialized* soft grippers whose morphology is tailored to the object’s features. Topology optimization offers a promising approach for producing specialized grippers, but its utility is limited by the requirement for pre-defined load cases. For soft grippers interacting with feature-rich objects, these loads arise from hundreds of unpredictable gripper-object contact forces during grasping and are unknown *a priori*. To address this problem, we introduce *SimTO*, a framework that enables high-resolution topology optimization by automatically extracting load cases from a contact-based physics simulator, eliminating the need for manual load specification. Given an arbitrary feature-rich object, *SimTO* produces highly customized soft grippers with fine-grained morphological features tailored to the object geometry. Numerical results show our designs are not only highly specialized to feature-rich objects, but also generalize to unseen objects.

Keywords: topology optimization, soft grippers, compliant mechanisms, design-dependent loads

1 Introduction

Soft robotic grippers are typically designed as *generalists* intended to handle a variety of objects (Brown et al. 2010; Ilievski et al. 2011; Pfaff et al. 2011; Yi et al. 2025), while *specialist* designs tailored to a constrained set of objects are under-explored (Dzedzickis et al. 2024). However, most industrial soft grasping applications - including

fruit harvesting or repetitive pick-and-place operations in warehouses - target only a constrained set of objects (Dzedzickis et al. 2024), highlighting the need for specialist designs in industry. Furthermore, generalist designs often struggle to grasp *feature-rich* objects with high topological variability, including gears on automotive assembly lines, corals with fragile protrusions, and vegetables with branching structures like cauliflower and

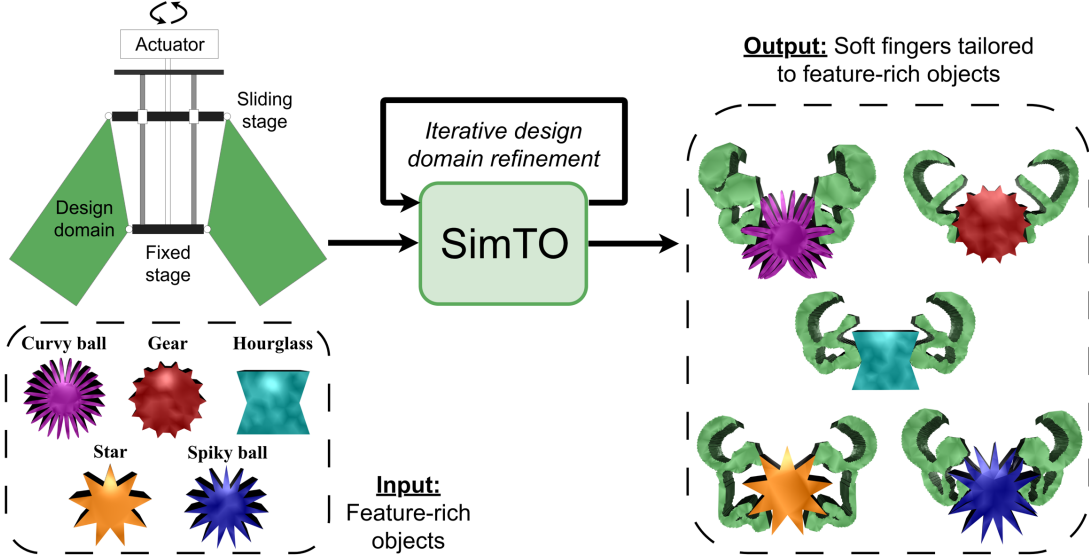


Fig. 1 The *SimTO* framework. **Left:** The inputs to *SimTO* include (i) a deformable, feature-rich object and (ii) a soft gripper whose dynamic grasping behaviour can be simulated. In this work, we used a soft gripper design scheme inspired by Liu et al. (2018), whose end-effectors are *soft fingers* actuated by the compression of a sliding stage. **Right:** Given an arbitrary feature-rich object, *SimTO* generates bespoke soft fingers which conform to that object’s shape under actuation.

broccoli. These limitations highlight the need for a design framework capable of generating specialist soft grippers for feature-rich objects.

Designing specialist soft grippers for feature-rich objects is challenging because it requires detailed knowledge of the contact interactions between the gripper and object (Birglen et al. 2008) - data that is often difficult or infeasible to obtain. Topology optimization (TO) is a powerful structural design framework and a strong candidate for producing specialized soft grippers (Bendsøe and Sigmund 2004), but its utility is limited by the requirement for pre-defined load cases. For soft grippers interacting with feature-rich objects, these loads arise from hundreds of unpredictable gripper-object contact forces during grasping and are unknown *a priori*. Recently, parametric optimization approaches have emerged which accurately model rich gripper-object contact forces (Gjoka et al. 2024; Yi et al. 2025). However, few works incorporate these contact forces into their optimization objective, and many use simple design parameterizations that hinder the generation of designs with diverse features.

In response, we introduce *SimTO*, a framework that enables high-resolution topology optimization by automatically extracting load cases from a contact-based physics simulator, overcoming the need for *a priori* load specification. This approach

is particularly advantageous for problems where rich load cases are difficult to obtain. Our **key contributions** are summarized as follows:

- We present a novel framework called *SimTO* that enables high-resolution topology optimization by automatically extracting load cases from a physics simulator, eliminating the need for *a priori* load specification.
- For problems involving design-dependent loads, *SimTO* enables an iterative optimization process that continually refines both the design and its corresponding loads. By repeatedly alternating between simulation-based load extraction and topology optimization, we incrementally arrive at highly specialized soft grippers for feature-rich objects.
- Further experimentation demonstrates that our specialized soft gripper designs possess a strong ability to generalize to out-of-domain objects.

2 Literature Review

Computational design frameworks for soft grippers share four fundamental components: (i) a design representation, (ii) a simulation method for performance evaluation, (iii) an objective function, and (iv) an optimization algorithm (Pinskier et al. 2024a). Generally, a design representation

is defined as an N -dimensional vector of design variables, ρ , that characterizes the morphology of a soft gripper, while the set of all possible vectors ρ forms an N -dimensional *design space*. The performance of a design is evaluated in simulation and quantified by an objective function, $f(\rho)$, which is then extremized by either a gradient-based or gradient-free optimization algorithm. While gradient-based methods are efficient at finding local optima in high-dimensional design spaces, gradient-free methods offer fewer convergence guarantees (Pinskier et al. 2024a).

Both topology optimization and parametric optimization approaches can be used for soft gripper design, with each offering different strengths and weaknesses. Topology optimization is a powerful framework that uses gradient-based optimization to obtain locally optimal solutions within high-dimensional design spaces (Bendsøe and Sigmund 2004), making it a strong candidate for producing specialized soft grippers. Conversely, many parametric design approaches (Liu et al. 2022; Navarro et al. 2023; Yao et al. 2024; Navez et al. 2024) use gradient-free evolutionary algorithms to optimize only a limited set of design variables that adjust the overall shape of a gripper in a constrained manner, preventing the emergence of specialized designs with fine-grained features.

Within topology optimization, however, a critical limitation exists due to the finite element formulation that is typically used. In SIMP-based topology optimization (Solid Isotropic Material with Penalization), designs are represented as a 2D or 3D grid of finite elements (Bendsøe and Sigmund 2004). Each element e is assigned a design variable $\rho_e \in [0, 1]$, with $\rho_e = 1$ indicating solid material and $\rho_e = 0$ representing the absence of material. Design performance is evaluated using the finite element method, which crucially requires the pre-specification of boundary conditions and applied loads. In many applications, **these loads cannot be easily determined**. For example, when optimizing the internal structure of an aircraft wing, Aage et al. (2017) required rich load cases obtained from expensive NASA wind-tunnel experiments. Similarly, when designing soft grippers specialized for feature-rich objects, the true load cases are not known *a priori*.

To our knowledge, all soft grippers designed via topology optimization (Liu et al. 2018; Zhang et al. 2019; Caasenbrood et al. 2020; Wang et al.

2020; Liu et al. 2023; Pinskier et al. 2024b) have largely overlooked the complex, time-varying contact interactions that occur between the gripper and object during grasping. Instead, these works have used generic, manually prescribed ‘dummy’ loads (Frecker et al. 1999) that define fixed trajectories for grippers to deform along. To date, this generic dummy load approach has only produced generalist designs that lack the specialized morphological features needed to securely grasp feature-rich objects. To address this gap, we introduce *SimTO*, a framework that replaces generic, manually prescribed dummy loads with rich gripper-object contact forces automatically extracted from dynamic soft grasping simulations.

3 Method

SimTO is a design optimization algorithm for compliant mechanisms - flexible monolithic structures that achieve motion through elastic deformation under loading (Frecker et al. 1999). The framework is designed for mechanisms that experience time-varying, design-dependent contact forces while performing a specified task (e.g., grasping an object in the case of a gripper). Each SimTO iteration consists of three stages: (i) dynamic simulation of the structure’s rich contact behaviour, (ii) contact force extraction, and (iii) topology optimization using a contact-aware objective function (Fig. 2).

As the designs and hence simulated contact forces evolve with each solve, performing SimTO over multiple iterations yields increasingly specialized mechanisms. As shown in Fig. 2, simulating an initial design produces a set of contact forces which automatically define task-specific deformation directions for topology optimization. Simulating the updated design - whose morphology is now better adapted to the task - produces *new* contact interactions and, consequently, *new* deformation directions, leading to further morphological refinement. In the remainder of this section, we explain stages (i) - (iii) of SimTO in further detail.

3.1 Dynamic simulation

We used Taccel (Li et al. 2025) to perform dynamic soft grasping simulations, owing to its ability to accurately model time-dependent deformation and frictional contact among multiple

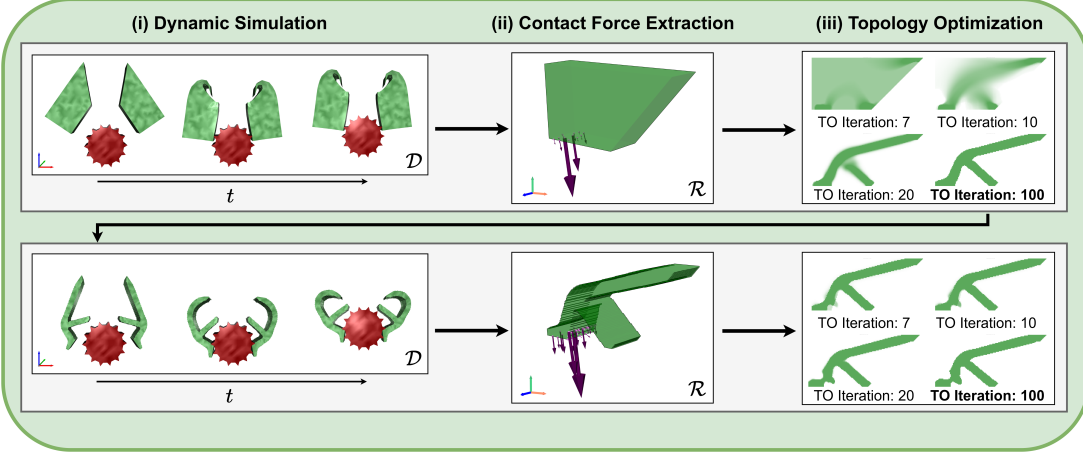


Fig. 2 *The SimTO method.* This figure shows two iterations of SimTO. Each iteration consists of: (i) a dynamic simulation of a 3D compliant mechanism in the deformed frame \mathcal{D} ; (ii) contact force extraction, where the simulated 3D forces are rotated into \mathcal{R} and projected onto the x - y plane; and (iii) topology optimization of the undeformed 2D design using these in-plane forces. The resulting 2D design is then extruded to initialize the next iteration.

interacting Neo-Hookean solids. Each simulation was initialized with the following gripper parameters: material stiffness E_g , Poisson's ratio ν_g , a tetrahedral mesh \mathcal{M}_g of the left soft finger with N_g nodes (later duplicated to form the right soft finger), and the initial gripper grasp pose \mathcal{P}_g . Analogous quantities were also defined for an arbitrary feature-rich object: E_o , ν_o , \mathcal{P}_o , and \mathcal{M}_o .

In each dynamic grasping simulation, the sliding stage of a soft robotic gripper (Fig. 1) was first compressed by d_c millimetres, and then the gripper was lifted by d_l millimetres. Each simulation lasted t seconds and consisted of N_t timesteps. During the first $t/2$ seconds, gripper compression was achieved by fixing the displacements of nodes on the fixed port of the design domain (Fig. 3) to 0, while input port nodes were compressed by $2d_c/N_t$ millimetres per timestep, resulting in a smooth compression of the sliding stage by d_c millimetres. In the final $t/2$ seconds, both input and output port nodes were lifted in the z -direction by $2d_l/N_t$ millimetres per timestep, corresponding to a smooth lifting of the entire gripper by d_l millimetres. In all examples presented in this paper, d_c was set to 80 mm, while ν_g and ν_o were 0.4.

3.2 Contact force extraction

In our work, dynamic simulations were performed in a deformed frame \mathcal{D} , while topology optimization was carried out in a 2D subspace of an undeformed frame \mathcal{R} (Fig. 2). In each simulation,

we first extracted a set of \tilde{N}_f contact forces, $\tilde{F} = \{\tilde{f}_1, \dots, \tilde{f}_{\tilde{N}_f}\}$, where each $\tilde{f}_i \in \mathbb{R}^3$ is a contact force vector expressed in \mathcal{R} . We then constructed a reduced set of $N_f \leq \tilde{N}_f$ two-dimensional forces, $F = \{f_1, \dots, f_{N_f}\}$, where each $f_i \in \mathbb{R}^2$ is used directly in topology optimization (Fig. 3). To understand how \tilde{F} was obtained - after which F followed naturally by a simple down-sampling procedure - it is useful to consider a single dynamic simulation, timestep by timestep.

At each timestep, contact forces were filtered to ensure they contributed to a secure grasp. Specifically, we only retained forces that (i) applied a positive normal force on the object and (ii) resisted slip. To implement this scheme, after each timestep we used the Kabsch algorithm (Kabsch 1976) to compute a rotation matrix that mapped 3D contact forces from \mathcal{D} to \mathcal{R} . We only kept forces with a negative y -component and a positive x -component in \mathcal{R} , corresponding to forces satisfying conditions (i) and (ii). To prevent our topology optimization objective function from being dominated by transient or weak contact forces, we used a magnitude-based update rule: if a force was already recorded for a specific gripper node, it was replaced by a newly detected force satisfying (i) and (ii) only if the new force had a larger magnitude. This procedure yielded the set of \tilde{N}_f gripper-object contact forces $\{\tilde{f}_1, \dots, \tilde{f}_{\tilde{N}_f}\}$.

To obtain the reduced set F from \tilde{F} , we first rounded the x -, y -, and z -coordinates of all \tilde{N}_f

contact points to the nearest millimetre. Because topology optimization was performed in the $x-y$ plane of \mathcal{R} , we grouped all 3D contact forces sharing a common (x, y) coordinate (i.e., forces lying along the same line of constant z). For each group, we averaged the 3D force vectors and subsequently set the z -component of the resulting vector to zero, yielding a 2D force vector \mathbf{f} located at (x, y) .

3.3 Topology optimization of a contact-aware objective function

Figure 3 shows the design domain, boundary conditions and simulated loads used to optimize a single soft finger. We used a conventional objective function for compliant mechanisms that simultaneously encourages designs with sufficient stiffness and deformability in user-specified directions (Frecker et al. 1999). However, whereas prior works manually specify a small number of generic deformation directions, we instead used our simulated contact forces $\{\mathbf{f}_1, \dots, \mathbf{f}_{N_f}\}$ to automatically define *object-specific* deformation directions.

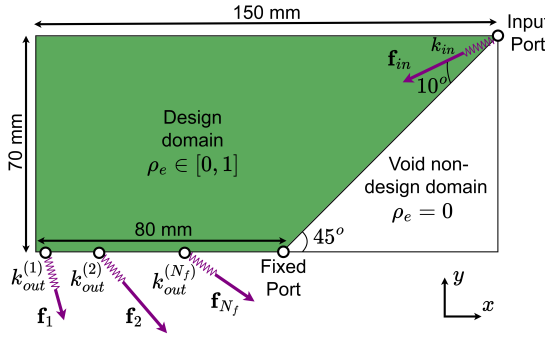


Fig. 3 Our design domain is based on that of Liu et al. (2018), but with three key differences. First, whereas they manually prescribed two dummy loads that encouraged designs to deform solely along the negative y -axis, ours deform along N_f simulated gripper-object contact force directions. Second, we rotated the input force \mathbf{f}_{in} by an additional 10° . Third, we did not enforce material retention along the lower 80mm edge of the design domain.

For each $\mathbf{f}_i \in \{\mathbf{f}_1, \dots, \mathbf{f}_{N_f}\}$, we maximized the mutual potential energy (MPE) associated with load i whilst minimizing its corresponding strain energy (SE) (Frecker et al. 1999). Maximizing the MPE for load i encourages deformation in the direction of \mathbf{f}_i at the associated (x, y) contact point within the design domain, whereas minimizing SE provides adequate stiffness under the

actuating input load (Frecker et al. 1999). In our work, the $150 \text{ mm} \times 70 \text{ mm}$ two-dimensional design domain from Fig. 3 was discretized into $150 \times 70 = 10,500$ square finite elements and a density-based TO approach was used (Bendsøe and Sigmund 2004). Each element e was assigned a material density ρ_e , and its Young's modulus was given by:

$$E(\rho_e) = E_{\min} + \rho_e^p (E_0 - E_{\min}), \quad (1)$$

where $\rho_e \in [0, 1]$, E_0 is the normalized material stiffness, $E_{\min} = 10^{-9}$ and $p = 3$. The global stiffness matrix $\mathbf{K}(\rho)$ was assembled from the element stiffness matrices, \mathbf{K}_e^0 , and a global stiffness matrix for numerical springs, \mathbf{K}_s , via:

$$\mathbf{K}(\rho) = \mathbf{K}_s + \sum_e E(\rho_e) \mathbf{K}_e^0 \quad (2)$$

where the matrix \mathbf{K}_s introduces standard numerical springs at the input and output ports of the design domain (Fig. 3), following common practice in compliant mechanism design, with spring constants $k_{\text{out}}^{(i)} = 0.1$ for $i = 1, \dots, N_f$ and $k_{\text{in}} = 0.1$. The full optimization problem was formulated as:

$$\begin{aligned} \underset{\rho}{\operatorname{argmax}} \quad f(\rho) &= \sum_{i=1}^{N_f} \|\mathbf{f}_i\| \frac{\text{MPE}_i}{\text{SE}_i} \\ &= \sum_{i=1}^{N_f} \|\mathbf{f}_i\| \frac{\mathbf{U}_i^T \mathbf{K}(\rho) \mathbf{U}_{\text{in}}}{\mathbf{U}_i^T \mathbf{K}(\rho) \mathbf{U}_i} \\ \text{subject to} \quad \frac{V(\rho)}{V_0} &= v_f, \\ \mathbf{K}(\rho) \mathbf{U}_{\text{in}} &= \mathbf{F}_{\text{in}}, \\ \mathbf{K}(\rho) \mathbf{U}_i &= \mathbf{F}_i, \quad i = 1, \dots, N_f. \end{aligned} \quad (3)$$

Here, \mathbf{f}_i refers to the i th simulated contact force in $\{\mathbf{f}_1, \dots, \mathbf{f}_{N_f}\}$, \mathbf{F}_i is the corresponding global force vector containing only this contact force and zeros elsewhere, and \mathbf{U}_i is the global displacement vector. The vector \mathbf{U}_{in} is the global displacement field produced by the input force vector \mathbf{F}_{in} , derived from the unit-magnitude force \mathbf{f}_{in} shown in Fig. 3. The terms $V(\rho)$ and V_0 represent the material volume and total design domain volume, respectively, and v_f is the target volume fraction.

We used a density filter to mitigate checkerboard patterns in optimized designs and encourage mesh-independent solutions (Andreassen et al.

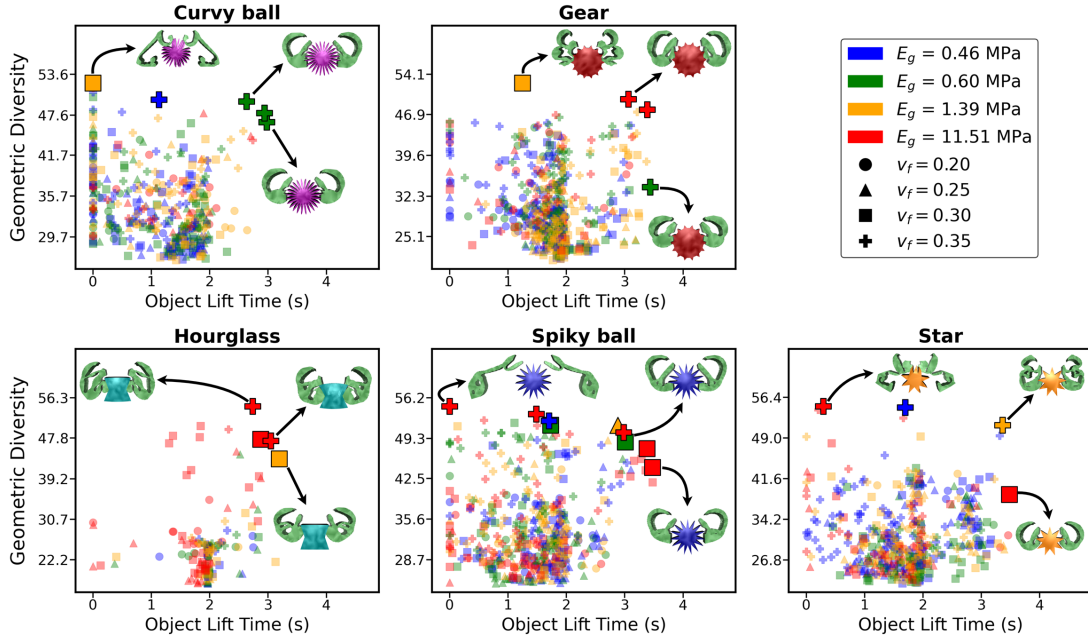


Fig. 4 Numerical results of SimTO optimization runs for the five feature-rich objects shown in Fig. 1. Each plot compares the geometric diversity and object lift time of all grippers. Designs on the resulting Pareto front are indicated by enlarged markers with black outlines.

2011), while the optimality criteria method (Bendsøe and Sigmund 2004) was used to solve (3). The framework outlined here was implemented in a Python-based optimization loop similar to that developed by Andreassen et al. (2011). In all examples presented in this paper, topology optimization was terminated when either the change in the material-density design variables fell below one percent or after 100 iterations. Because a single SimTO run may involve multiple rounds of topology optimization, this 100-iteration limit was imposed for computational efficiency. In most cases, this limit was sufficient to achieve high-performing designs.

4 Results

4.1 Generating object-specific soft grippers

Using SimTO, we generated 2071 bespoke soft grippers (Fig. 4) for five different feature-rich objects: a *curvy ball*, *gear*, *hourglass*, *spiky ball* and *star* (Fig. 1). For each object, we performed a parameter sweep across four volume fractions, $v_f \in \{0.20, 0.25, 0.30, 0.35\}$, and four 3D-printable material moduli for both the gripper and object,

$E_g, E_o \in \{0.46, 0.60, 1.39, 11.51\}$ MPa, resulting in 64 optimization runs per object. As variations in E_g , E_o and v_f can significantly impact the simulated gripper-object contact interactions - with E_g and E_o controlling the relative stiffness between the gripper and object, and v_f determining the gripper's total volume and geometry - we expected different optimization runs to yield designs with unique morphological features.

Each run concluded after 20 SimTO iterations or when two successive designs, ρ^i and ρ^{i+1} , satisfied the convergence criterion $\sum_e (\rho_e^{i+1} - \rho_e^i)^4 < \epsilon$. We set $\epsilon = 10$, an empirically determined value that ended the optimization once two consecutive SimTO iterations produced sufficiently similar designs. However, because the design-dependent nature of the optimization creates a highly nonlinear process, designs generated within a given SimTO run were not guaranteed to *monotonically* improve grasping performance. This meant 'converged' designs did not always possess the most effective features for specialized grasping. To capture the full range of high-performing designs, we analyzed the performance of all designs generated across every SimTO iteration (Fig. 4).

While the theoretical maximum number of designs per object was $64 \times 20 = 1280$, the

actual number of feasible designs generated was: 395 (curvy ball), 543 (gear), 149 (hourglass), 495 (spiky ball) and 489 (star). The hourglass geometry, being smoother than the ‘spikier’ objects, typically produced simpler contact force distributions, causing SimTO to converge in fewer than 3 iterations on average. For the remaining objects, SimTO converged in approximately 6 to 9 iterations on average. Note that an additional 245 infeasible designs - 10.6% of the total - were automatically excluded from the analysis, either because they had disconnected geometries or lacked material at the fixed port of the design domain. We attribute these spurious results to numerical instabilities caused by large displacements in low-stiffness elements - a well-documented problem in topology optimization (Pedersen et al. 2001).

In all optimization runs, the design domain from Fig. 3 was used as the initial simulated design. Dynamic grasping simulations spanned $t = 4s$, where grippers were first compressed by $d_c = 80\text{ mm}$ during the first two seconds, before being lifted $d_l = 30\text{ mm}$. Across all SimTO iterations, the initial gripper grasp pose \mathcal{P}_g and object pose \mathcal{P}_o remained constant. Maintaining fixed poses was not mandatory, and we hypothesize that strategically varying \mathcal{P}_g and \mathcal{P}_o would produce morphologies that are robust to object and gripper positioning uncertainty, rather than generating designs that are specialized to a single gripper-object pose combination.

4.2 Analyzing the trade-off between geometric diversity and object lift time

The relationship between *geometric diversity* and *object lift time* for all generated designs is illustrated in Fig. 4. For each feature-rich object, the geometric diversity of the i th design was defined as $D_i = \|\boldsymbol{\rho}_i - \bar{\boldsymbol{\rho}}\|$, where $\bar{\boldsymbol{\rho}} = \frac{1}{K} \sum_{i=1}^K \boldsymbol{\rho}_i$ represents the mean morphology of the K designs produced for that object. In this case, higher geometric diversity values correspond to designs that deviate significantly from the mean morphology. We used *object lift time* as a proxy for functional performance, which was defined as the total duration that the object was simultaneously in contact with the gripper while not touching the ground during simulation.

As shown in Fig. 4, designs located on the Pareto front typically used a high volume fraction of 0.30 or 0.35. Only the spiky ball had one Pareto-optimal design with $v_f = 0.25$. This trend was expected, as a larger material budget gives the optimizer the freedom to generate more exotic morphologies with greater geometric diversity. Furthermore, higher volume designs are capable of generating larger contact forces, and are expected to increase object lift times due to their increased grip strength.

While high geometric diversity often signals novel features tailored for specialized grasping, it can also indicate the presence of excessive or redundant features. This is evident in the curvy ball, spiky ball and star results (Fig. 4), where the most geometrically diverse designs developed long “dead-weight” appendages that dragged along the ground without contributing to grasping. Conversely, while designs with the highest lift times often possessed less diverse features that were functionally more useful, in some cases these designs demonstrated overfitting to the specific gripper-object pose combination used during optimization. Interestingly, designs located slightly off the Pareto front with relatively high object lift times and geometric diversity often possessed the most useful morphological features for **robust** and secure grasping, which we explicitly demonstrate in the next section.

4.3 Evaluating the specificity and generality of twenty designs

From the results presented in Fig. 4, we manually selected twenty specialized designs for further evaluation, including ten *soft* designs (Fig. 5) optimized with $E_g = 11.51\text{ MPa}$ and ten *softer* designs (Fig. 6) optimized with lower elastic moduli $E_g \in \{0.46, 0.60, 1.39\}\text{ MPa}$. We selected two designs per object for both the “soft” and “softer” groups.

In-domain and out-of-domain grasping performance were evaluated for all designs, with $E_g = E_o = 11.51\text{ MPa}$ for all *soft* designs, and $E_g = E_o = 0.46\text{ MPa}$ for all *softer* designs. For in-domain testing, we performed 35 simulated grasps per design on the object for which it was optimized. Seven object poses \mathcal{P}_o were used: rotations of 5° and 10° about the z -axis; translations of 6 mm and 12 mm along the x -axis; translations of

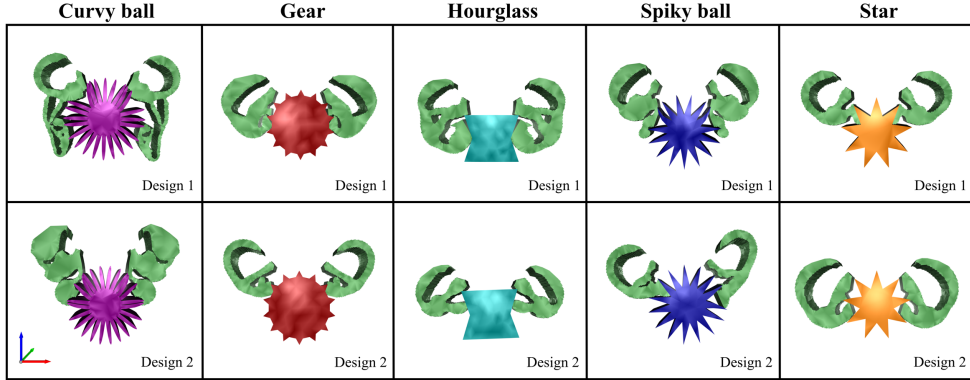


Fig. 5 *Ten soft designs.* All designs were optimized with $E_g = 11.51$ MPa and evaluated with E_g and E_o also equal to 11.51 MPa (see Table 1 for results). In this figure, each design is compressed by $d_c = 80$ mm.

Table 1 *Results for ten soft designs.* Performance is evaluated for each design from Fig. 5, with E_g and E_o set to 11.51 MPa during evaluation.

Object	Design	E_g (Opt.)	E_o (Opt.)	v_f (Opt.)	Iters. (Opt.)	In-domain Object Stress (Pa)	In-domain Success	Out-of-domain Success
Curvy ball	1	11.51	0.46	0.25	4	$(7.42 \pm 1.61) \times 10^5$	80.00%	89.29%
	2	11.51	0.46	0.35	2	$(9.77 \pm 2.53) \times 10^5$	74.29%	71.43%
Gear	1	11.51	1.39	0.35	5	$(2.03 \pm 0.59) \times 10^5$	91.43%	77.86%
	2	11.51	11.51	0.20	9	$(1.20 \pm 0.22) \times 10^5$	88.57%	82.14%
Hourglass	1	11.51	0.46	0.35	5	$(1.07 \pm 0.25) \times 10^5$	94.29%	76.43%
	2	11.51	1.39	0.20	2	$(1.34 \pm 0.41) \times 10^5$	85.71%	89.29%
Spiky ball	1	11.51	0.46	0.30	6	$(7.80 \pm 4.09) \times 10^5$	74.29%	82.14%
	2	11.51	1.39	0.20	4	$(4.36 \pm 1.49) \times 10^5$	71.43%	89.29%
Star	1	11.51	1.39	0.20	1	$(1.88 \pm 0.17) \times 10^5$	85.71%	84.29%
	2	11.51	11.51	0.30	2	$(4.25 \pm 1.09) \times 10^5$	85.71%	87.86%

8 mm and 16 mm along the y -axis, and the unper- turbed origin pose (i.e., the pose shown for each object in Fig. 5). Each pose was evaluated in five independent trials with distinct random seeds. For out-of-domain testing, designs optimized for a specific object were evaluated on four previously unseen objects, performing 35 grasps per unseen object (again using five trials for each of the seven object poses).

During evaluation, each simulated grasp lasted $t = 8$ s, with the first 4 s used to compress the sliding stage by $d_c = 80$ mm, and the remaining time used to lift the gripper by 40 mm. A grasp was considered successful if, at the end of the simulation, the object remained in contact with the gripper while not touching the ground. During in-domain tests, peak von Mises stresses were recorded for

the objects being grasped. Tables 1 and 2 summarize the in-domain and out-of-domain performance of the “soft” and “softer” designs respectively. All in-domain results are averages over 35 independent grasps, and out-of-domain success rates are based on 140 grasps across four unseen objects. Note that these tables also show the actual values of E_g , E_o and v_f used during optimization, indicated in brackets as “Opt.” - not to be confused with the evaluation values of E_g and E_o) and the number of SimTO iterations, indicated as “Iters.”

4.3.1 Grasping performance of soft designs

All soft designs achieved high in-domain and out-of-domain grasping success (Table 1), suggesting that these specialist grippers generalize well to

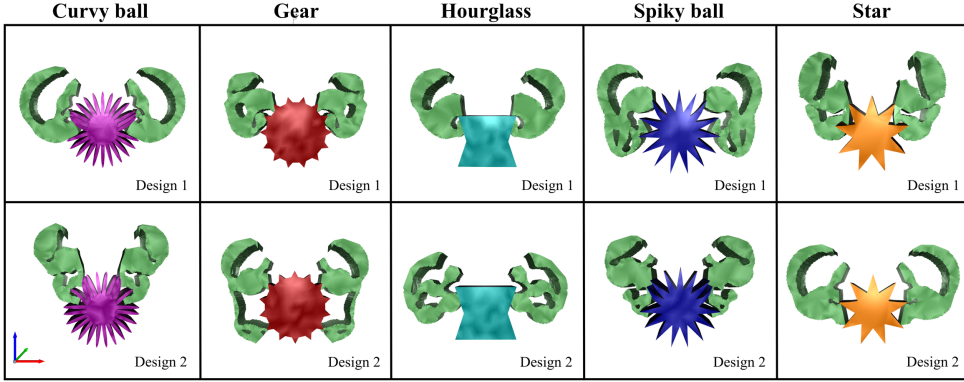


Fig. 6 *Ten softer designs.* All designs were evaluated with E_g and E_o set to 0.46 MPa (see Table 2). In this figure, each design is compressed by $d_c = 80$ mm.

Table 2 *Results for ten softer designs.* Performance is evaluated for each design from Fig. 6, with E_g and E_o set to 0.46 MPa during evaluation.

Object	Design	E_g (Opt.)	E_o (Opt.)	v_f (Opt.)	Iters. (Opt.)	In-domain Object Stress (Pa)	In-domain Success	Out-of-domain Success
Curvy ball	1	0.60	11.51	0.35	7	$(3.37 \pm 0.63) \times 10^4$	71.43%	75.00%
	2	0.60	0.60	0.35	4	$(5.71 \pm 1.44) \times 10^4$	71.43%	70.71%
Gear	1	0.60	0.46	0.35	19	$(1.16 \pm 0.21) \times 10^4$	71.43%	78.57%
	2	1.39	0.60	0.35	1	$(1.31 \pm 0.40) \times 10^4$	71.43%	60.71%
Hourglass	1	1.39	0.60	0.30	2	$(1.04 \pm 0.27) \times 10^4$	71.43%	71.43%
	2	0.60	11.51	0.25	3	$(3.40 \pm 0.32) \times 10^3$	71.43%	60.00%
Spiky ball	1	0.46	0.46	0.35	3	$(2.60 \pm 0.69) \times 10^4$	71.43%	67.86%
	2	1.39	0.46	0.35	10	$(4.28 \pm 1.83) \times 10^4$	57.14%	71.43%
Star	1	0.46	0.46	0.35	11	$(4.88 \pm 1.56) \times 10^4$	71.43%	46.43%
	2	0.46	1.39	0.35	13	$(2.07 \pm 0.48) \times 10^4$	71.43%	60.71%

unseen objects in varying poses. These designs demonstrated five of the six unique grasping strategies identified in our work (Fig. 7): (1) *multi-cavity grasping* (e.g., the second star design), where multiple cavities are developed for object protrusions to slot into; (2) *multi-arm grasping* (e.g., the first curvy ball and hourglass designs), where designs use multiple appendages to secure objects at several sites; (3) *hook grasping* (e.g., the second curvy ball and first spiky ball design), where designs develop hooks that firmly encase object protrusions; (4) *cookie cutter grasping* (e.g., the first gear design), where grippers deform to perfectly match the complex geometries of their target objects and maximize contact area; and (5) *pinch grasping* (all remaining designs), where elongated end-effectors apply large normal forces

on objects. While most designs required multiple SimTO iterations to develop their features, some high-performing designs were achieved in as few as 1 or 2 SimTO iterations (e.g., the second hourglass and both star designs). However, two of these designs were less geometrically diverse ‘pinch’ grippers.

4.3.2 Grasping performance of softer designs

The softer designs returned slightly lower success rates compared to the stiffer designs from Table 1. This trend was expected, as reduced material stiffness inherently decreases overall grip strength. Despite this, the grippers maintained strong generalization capabilities. The most robust generalizers used multi-arm (e.g., the first hourglass and

gear designs), multi-cavity (e.g., the first curvy ball design) and hook-based (e.g., the second spiky ball design) grasping strategies. Interestingly, multi-armed designs with high geometric diversity were obtained in as few as 1 and 2 SimTO iterations (e.g., the second gear and first hourglass designs). This suggests that the use of rich contact-based loads alone can generate high-performing specialist grippers, and multiple SimTO iterations are not always required.

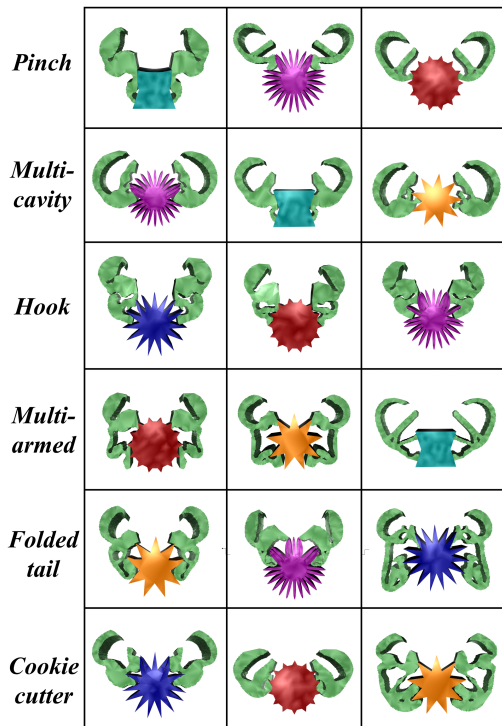


Fig. 7 Six different soft grasping strategies discovered by *SimTO*, with three examples shown per strategy.

5 Discussion

5.1 Diverse grasping strategies

We used SimTO to discover six different grasping strategies (Fig. 7). While (1) *multi-cavity*, (2) *multi-arm*, (3) *hook*, (4) *pinch* and (5) *cookie cutter* grasps were previously described in Sec. 4.3.1, we also discovered designs with (6) *folded tail* grasps. These designs developed an upper palm and a lower tail that could fold inward to carry

objects from underneath (Fig. 7). We emphasize that these categories are not mutually exclusive. For example, folded tail designs can be viewed as multi-armed designs with an inward-folding lower arm, while cookie cutter designs could be viewed as multi-cavity designs that conform perfectly to feature-rich geometries.

5.2 Developing useful automatic design-selection criteria

In Sec. 4.3, we manually selected specialist designs with diverse grasping modes for evaluation. However, improving SimTO further will require *automatic design-selection criteria* capable of identifying high-performing designs for arbitrary objects.

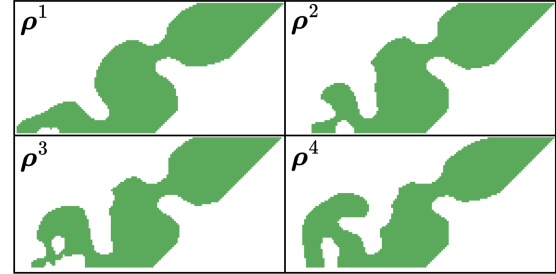


Fig. 8 Four candidate designs generated when optimizing the second curvy ball design (i.e., ρ^4) from Fig. 6.

To illustrate the challenge of developing such criteria, consider the four designs (Fig. 8) produced by SimTO when optimizing the second curvy ball design in Fig. 6. We manually selected ρ^4 for evaluation because it has a hooking mechanism that is well-suited to the object’s curved geometry. However, soft robotic grippers deform and interact with objects in non-intuitive ways, meaning manual selection risks overlooking high-performing designs that use unconventional grasping modes. Conversely, selecting designs solely for geometric diversity could elevate a design such as ρ^3 , which is geometrically diverse but performs poorly. Thus, robust automatic selection methods which balance geometric diversity with functional performance are needed.

6 Conclusion

There are several promising directions for meaningful future work. First, SimTO could be used

to independently optimize both end-effectors of a soft gripper rather than one, which could lead to asymmetric grippers with novel grasping strategies. Second, 3D topology optimization could be used to generate new designs with features that are unattainable with a 2D formulation. Third, the gripper grasp pose and object pose could be strategically varied during design optimization to create designs that are more robust to object and gripper positioning uncertainty. Finally, we plan to fabricate and experimentally validate the designs presented here. As we continue to improve SimTO, we believe it will enable the automated design of increasingly specialized soft robotic grippers for a broad range of real-world applications.

Declarations

Author contributions. All authors contributed to the study conception and design. Material preparation, data collection and analysis were performed by Kurt Enkera. The first draft of the manuscript was written by Kurt Enkera and all authors commented on previous versions of the manuscript. All authors read and approved the final manuscript.

Conflict of interest. We have no conflict of interest to report.

Data availability. All designs presented in this paper are available at: <https://github.com/kurtenkera/SimTO-Dataset>.

Replication of results. The results presented in this paper can be replicated by implementing the methods outlined in Sections 3 and 4.

Funding. Not applicable.

Ethics approval and consent to participate. Not applicable.

References

Aage N, Andreassen E, Lazarov BS, et al (2017) Giga-voxel computational morphogenesis for structural design. *Nature* 550(7674):84–86. <https://doi.org/10.1038/nature23911>, URL <https://doi.org/10.1038/nature23911>

Andreassen E, Clausen A, Schevenels M, et al (2011) Efficient topology optimization in matlab using 88 lines of code. *Structural and Multi-disciplinary Optimization* 43(1):269–278. <https://doi.org/10.1007/s00158-010-0594-7>

Bendsøe MP, Sigmund O (2004) *Topology Optimization: Theory, Methods, and Applications*, 2nd edn. Springer Berlin Heidelberg, <https://doi.org/10.1007/978-3-662-05086-6>

Birglen L, Laliberté T, Gosselin C (2008) *Underactuated Robotic Hands*, 1st edn. Springer Tracts in Advanced Robotics, Springer Berlin, Heidelberg, <https://doi.org/10.1007/978-3-540-77459-4>

Brown E, Rodenberg N, Amend J, et al (2010) Universal robotic gripper based on the jamming of granular material. *Proceedings of the National Academy of Sciences* 107(44):18809–18814. <https://doi.org/10.1073/pnas.1003250107>, URL <https://www.pnas.org/doi/abs/10.1073/pnas.1003250107>

Caasenbrood B, Pogromsky A, Nijmeijer H (2020) A computational design framework for pressure-driven soft robots through nonlinear topology optimization. In: 2020 3rd IEEE International Conference on Soft Robotics (RoboSoft), pp 633–638, <https://doi.org/10.1109/RoboSoft48309.2020.9116010>

Dzedzickis A, Petronienė JJ, Petkevičius S, et al (2024) Soft grippers in robotics: Progress of last 10 years. *Machines* 12(12). <https://doi.org/10.3390/machines12120887>, URL <https://www.mdpi.com/2075-1702/12/12/887>

Frecker M, Kikuchi N, Kota S (1999) Topology optimization of compliant mechanisms with multiple outputs. *Structural Optimization* 17(4):269–278. <https://doi.org/10.1007/BF01207003>

Gjoka A, Knoop E, Bächer M, et al (2024) Soft pneumatic actuator design using differentiable simulation. In: ACM SIGGRAPH 2024 Conference Papers. Association for Computing Machinery, New York, NY, USA, SIGGRAPH '24, <https://doi.org/10.1145/3641519.3657467>, URL <https://doi.org/10.1145/3641519.3657467>

Ilievski F, Mazzeo AD, Shepherd RF, et al (2011) Soft robotics for chemists. *Angewandte Chemie* 123(8):1930–1935. <https://doi.org/https://doi.org/10.1002/ange.201006464>, URL <https://onlinelibrary.wiley.com/doi/abs/10.1002/ange.201006464>

Kabsch W (1976) A solution for the best rotation to relate two sets of vectors. *Acta Crystallographica Section A* 32(5):922–923. <https://doi.org/10.1107/S0567739476001873>

Li Y, Du W, Yu C, et al (2025) Taccel: Scaling up vision-based tactile robotics via high-performance gpu simulation. URL <https://arxiv.org/abs/2504.12908>, arXiv:2504.12908

Liu CH, Chen TL, Chiu CH, et al (2018) Optimal design of a soft robotic gripper for grasping unknown objects. *Soft Robotics* 5(4):452–465

Liu CH, Yang SY, Shih YC (2023) Optimal design of a highly self-adaptive gripper with multi-phalange compliant fingers for grasping irregularly shaped objects. *IEEE Robotics and Automation Letters* 8(11):7026–7033. <https://doi.org/10.1109/LRA.2023.3313877>

Liu J, Low JH, Han QQ, et al (2022) Simulation data driven design optimization for reconfigurable soft gripper system. *IEEE Robotics and Automation Letters* 7(2):5803–5810. <https://doi.org/10.1109/LRA.2022.3155825>

Navarro SE, Navez T, Goury O, et al (2023) An open source design optimization toolbox evaluated on a soft finger. *IEEE Robotics and Automation Letters* 8(9):6044–6051. <https://doi.org/10.1109/LRA.2023.3301272>

Navez T, Liévin B, Peyron Q, et al (2024) Design optimization of a soft gripper using self-contacts. In: 2024 IEEE 7th International Conference on Soft Robotics (RoboSoft), pp 1054–1060, <https://doi.org/10.1109/RoboSoft60065.2024.10521925>

Pedersen CBW, Buhl T, Sigmund O (2001) Topology synthesis of large-displacement compliant mechanisms. *International Journal for Numerical Methods in Engineering* 50(12):2683–2705. <https://doi.org/https://doi.org/10.1002/>

nme.148

Pfaff O, Simeonov S, Cirovic I, et al (2011) Application of finray effect approach for production process automation. In: *Annals & Proceedings of DAAAM International*, pp 1247–1249

Pinskier J, Wang X, Liow L, et al (2024a) 12 - automated design of 4d-printed soft robots. In: Zolfagharian A, Bodaghi M (eds) *Smart Materials in Additive Manufacturing, Volume 3. Additive Manufacturing Materials and Technologies*, Elsevier, p 303–328, <https://doi.org/https://doi.org/10.1016/B978-0-443-13673-3.00012-2>, URL <https://www.sciencedirect.com/science/article/pii/B9780443136733000122>

Pinskier J, Wang X, Liow L, et al (2024b) Diversity-based topology optimization of soft robotic grippers. *Advanced Intelligent Systems* 6(4):2300505. <https://doi.org/https://doi.org/10.1002/aisy.202300505>

Wang R, Zhang X, Zhu B, et al (2020) Topology optimization of a cable-driven soft robotic gripper. *Structural and Multidisciplinary Optimization* 62(5):2749–2763. <https://doi.org/10.1007/s00158-020-02619-y>

Yao Y, He L, Maiolino P (2024) Spada: A toolbox of designing soft pneumatic actuators for shape matching based on surrogate modeling. *Robotics Reports* 2(1):1–14. <https://doi.org/10.1089/rorrep.2023.0029>, PMID: 39263556, <https://doi.org/10.1089/rorrep.2023.0029>

Yi S, Bai X, Singh A, et al (2025) Co-design of soft gripper with neural physics. In: Lim J, Song S, Park HW (eds) *Proceedings of The 9th Conference on Robot Learning, Proceedings of Machine Learning Research*, vol 305. PMLR, pp 4313–4327, URL <https://proceedings.mlr.press/v305/yi25a.html>

Zhang H, Kumar AS, Chen F, et al (2019) Topology optimized multimaterial soft fingers for applications on grippers, rehabilitation, and artificial hands. *IEEE/ASME Transactions on Mechatronics* 24(1):120–131. <https://doi.org/10.1109/TMECH.2018.2874067>